Punctuated Plume Penetration: Entrainment Dynamics of the Layered Filling Box

Yana Bebieva

October 15, 2015

1 Introduction

Many field observations indicate a layered stratification in the Global Ocean. For example, double-diffusive staircase structures are prevalent across the Arctic Ocean inhibiting different depth regions: above the Atlantic Water layer at around 400 m and in the deep Arctic above the homogeneous bottom layer. There are proposed scenarios on how brine-enriched shelf water plumes can penetrate towards the deep Arctic (see e.g., [1, 2]) causing slow deep water ventilation. Presumably, while descending such dense plumes pass through the regions of a layered stratification that can modify the plume dynamics. The influence of the layered stratification on plume dynamics and a feedback mechanisms have not been investigated yet.

Another example where plume interacts with the layered stratification is melting of marine-terminating glaciers. Recently it has been shown that glacial melting rate can be constrained by considering interaction of turbulent plume with a linearly stratification in a presence of repeating layered intrusions [11].

In this study by conducting a series of experiments and using the numerical model, we examine how layered stratification can change the plume dynamics and how plume can modify the initial stratification.

This report is organized as follows. In the next section, we describe the experimental technique. We describe the observed dynamics of plume penetration through the stratified environment and interaction with the layers in section 2.2. In section 3, we present the developed numerical model and discuss model outputs. Findings are summarized and discussed in section 4.

2 Experiments

2.1 Experimental procedure

We have conducted a series of experiments to understand the interaction between layered stratification and a turbulent plume. In these experiments we used: a square tank (42 cm $\times$ 42 cm $\times$ 70 cm), a plume source, a conductivity–temperature (CT) probe and a light projector and a camera to create shadowgraph images (Figure 1).

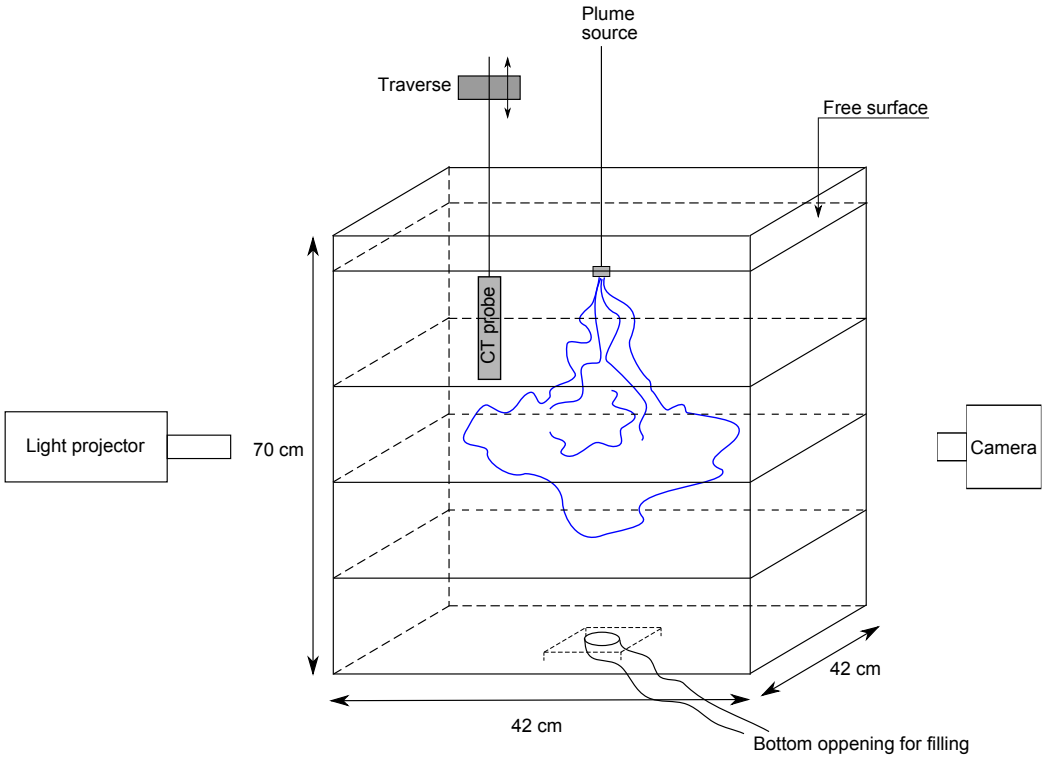

Figure 1: A schematic of the experimental set-up showing a square tank with layered stratification. Blue line shows a salt solution plume, released in the middle of the tank. Evolution of stratification is measured by a traversing conductivity–temperature (CT) probe from the depth where a plume released till maximum depth CT probe can reach, covering the total depth of about 30 cm. This schematic shows the initial stage of the experiment when the plume has been just released and depth of the free surface corresponds to the location of the plume source.

To establish a layered stratification we prepared solutions with different density (i.e., salinity) and fill the tank through a bottom opening layer by layer starting with fresh water and using a very low flow rate to reduce turbulent mixing and create sharp interfaces. The bottom opening was covered by an elevated metallic plate to spread incoming flow horizontally. With such technique an average height of interfaces is about 1–1.5 cm. We used one value of bulk stratification $N_0 \approx 1.13$ s^{-1}, apply two different flow rates ($Q_1 \approx 0.95$ cm^3/s and $Q_2 \approx 1.9$ cm^3/s) and choose three layer depths of 10 cm, 5 cm and 2.5 cm (that becomes effectively a linear stratification after some time due to diffusive mixing). In total we had 6 experiments.

Salt solution plumes (with 20% salinity) were released in the middle of the tank and the CT probe was located at a diagonal position about 1/4 from one of the corners in order to sample density evolution in time and not to have influence from turbulent mixing due to plume propagation. CT measurements have a vertical resolution of ~ 0.6 mm and only down-going profiles were used in the analysis because the CT sensors are located at the base of the profiler so that they are affected by turbulence in the wake of the instrument

in the up-cast profiles. The total profiled depth is about 30 cm, spanning from the depth where a plume is released till ∼20 cm from the bottom of the tank. It takes ∼90 s to finish one cycle of sampling.

In addition to the data derived from the CT measurements we used shadowgraph technique of the flow pattern visualization. Pictures were taken every 30 seconds, allowing to sample the first front propagation with 3 times higher frequency compared to the CT measurements. We used the Hough transform [8] to identify locations of interfaces in each image and calculate rate of first front descent. This method allows to distinguish only well-separated interfaces. At the moments when an interface reaches the one bellow its location is no longer recognizable and there are some missing data. Signal reappears again when this bottom interface starts to move downwards from its original position (see Figure 2).

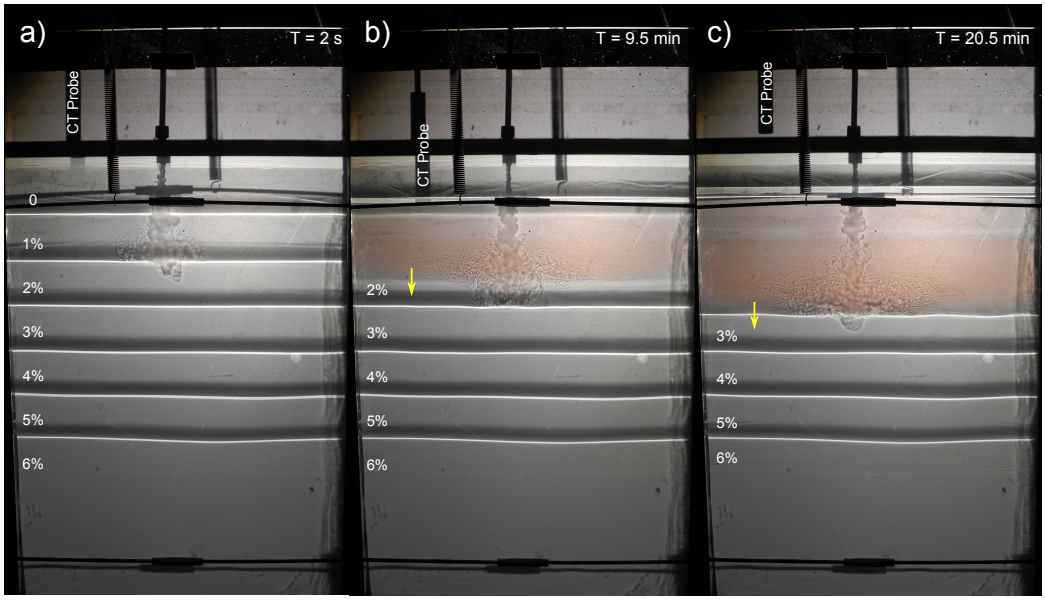

Figure 2: Shadowgraph (corresponding to the experiment $N_0 \approx 1.13$ s^{-1}, $Q_0 \approx 1.9$ cm^3/s, $h = 5$ cm) showing evolution of the background stratification due to interaction with the dense (salinity of 20%) plume at a) 2 s, b) 9.6 min and c) 20.5 min after the beginning of the experiment. Salinity is marked in percentage for each layer. Yellow arrows represent a direction of the first front propagation. Reddish color shows contaminated fluid. An uncontaminated layer (see text) is visible in c).

2.2 Experimental results

2.2.1 Qualitative observations

In order to examine the impact of plume on layered stratification, we begin by characterizing the qualitative observations of mixing within the layers and at the interface.

After a plume has been released, it entrains ambient fluid as it descends. Depending on the initial buoyancy flux the plume can pass through a few layers (interfaces) before the buoyancy flux becomes zero (at the depth z_F, note that at the very first moment of

the experiment this level always coincides with one of the artificially created interfaces) and then it spreads out laterally. Some portion of the plume, however, penetrate further till the depth where momentum flux is zero (z_M, this level does not necessarily coincide with an interface as shown in Figure 3, see e.g., Figure 2a, 2c). In the overshooting region (depth range between z_F and z_M) penetrative entrainment process is taking place and the plume fluid is mixes with the more dense ambient fluid beneath z_F. This mixture eventually ascends towards its neutral density level that is close to z_F but bellow this depth. Thus, the penetrative entrainment modifies the ambient stratification by introducing lighter fluid in place of the original dense fluid within the mixed layer (Figure 4a). Depth where the ambient stratification (after some time from the beginning of the experiment) begins to differ from the original is defined as a penetrative depth (z_p) of the descending front (Figure 3,4). The other process that happens as the plume fluid spreads out at z_F is a formation of a stable stratification above this level according to a "filling box" model described by [3].

As time evolves, a plume head in an overshooting region reaches the next artificial interface and entrains even more dense fluid from the layer below that interface (as shown in Figure 3). This accelerates the propagation rate of the descending front, since each time portion of the dense fluid in the final mixture due to penetrative entrainment increases and neutral density level is moving downward faster compared to the previous stage when penetrative entrainment operates only within the mixed layer. Meanwhile, due to the filling box process density of the plume fluid at z_F increases and z_F approaches z_P. At the moment when $z_F = z_P$, the density of the plume fluid becomes equal to the density of a remainder portion of the initial mixed layer and the plume punches through this remnant towards the next artificial interface leaving behind an uncontaminated background fluid (Figure 3, 4a).

This process continues, however, only first ~ 2 uncontaminated layers are formed as the remainders from the initial mixed layers. When plume propagates deeper z_F can not catch up with z_P any more, because it takes a longer time to accumulate density through a filling box mechanism and penetrative entrainment takes over and erodes the background stratification in a way, that every time when z_P approaches an artificial interface an actual jump in density is even larger than it was in the original stratification (Figure 4b).

2.2.2 Quantitative observations

It is of interest to examine the variations in center of mass of the contaminated fluid and the rate of the descending front across the set of experiments. The center of mass can be expressed as

$$Z_{CM} = \frac{\int(\rho(z,t) - \rho(z,0))z dz}{\int(\rho(z,t) - \rho(z,0))dz}, \tag{1}$$

where $\rho(z,0)$ is density at the beginning of the experiment ($t = 0$) and $\rho(z,t)$ is density after some time, z is the vertical coordinate. Figure 5 indicates that data from all experiments fall around the same curve showing that during the first instants the center of mass moves towards the plume source because all added plume fluid is accumulated within the top layers. Later in time, when the plume fluid is transported down into deeper regions, the center of mass begins to move away from the plume source. The descend rate of center of

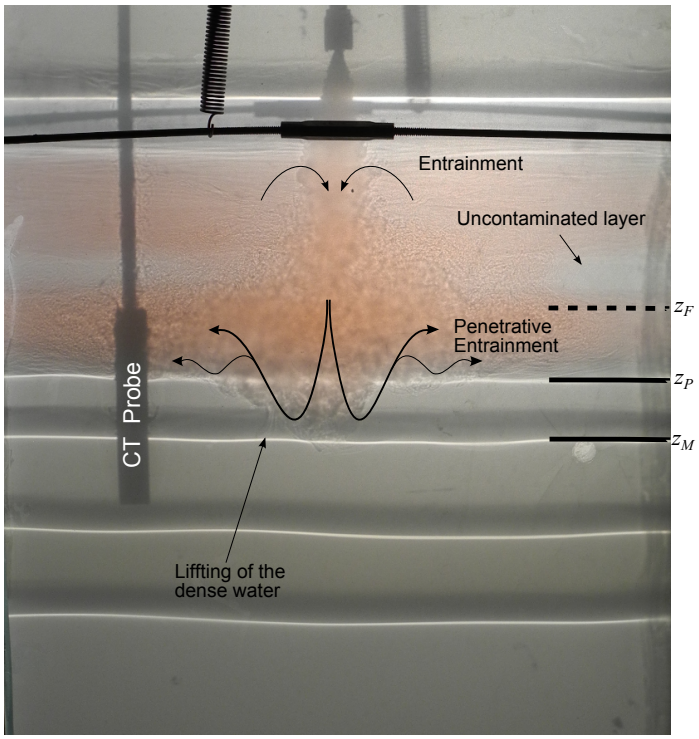

Figure 3: Example of a shadowgraph image showing two different types of mixing of plume fluid with the ambient water: entertainment from the sides of the plume and penetrative entertainment from the base of the plume). Uncontaminated layer is moving upward (see text for details). Location of the penetration depth (z_P), the depth where momentum flux is zero (z_M) are shown by solid black lines and approximate location of the depth where buoyancy flux is zero (z_F) is shown by dashed line.

mass is about the same for all experiments, meaning that layered stratification does not influence the the bulk property of the propagation of the contaminated fluid within the basin.

To compute the second important measure of the distribution of contaminated fluid in the basin, the descend rate of the penetration level, we used data derived from shadowgraph images (as described in section 2.1). The rate of penetration of the descending front in the experiments with a linear stratification (Figure 6) follows $t^{1/2}$ that is in agreement with "stratified filling box" experiments performed by [5], where continuous linear stratification was used. In the experiments with the layered stratification, z_p descends with a changing rate depending on the region of the profile where penetrative entrainment takes place. When ambient fluid entrains only from one mixed layer, z_P propagates very slowly, however, once the penetrative entrainment encompasses some portion of the layer below (in other words, when z_M crosses next artificial interface), the descend rate increases. At the early stages of the experiment (Figure 6, at time around 5 and 9) the plume punches through the remnant of the original layer as described in section 2.2.1 and a jump in propagation of z_P is observed. Note that the depth of this jump may contain some artificial signal due to the method we

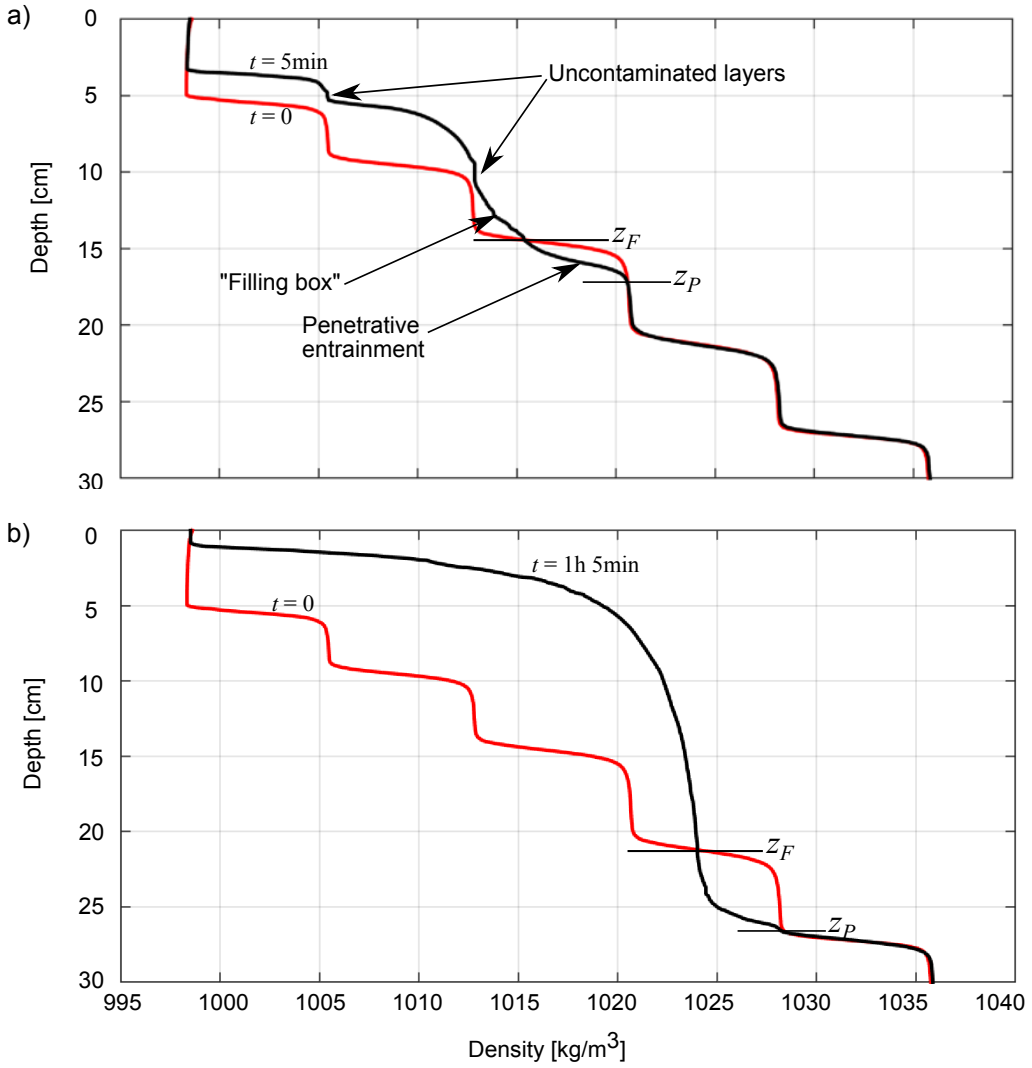

Figure 4: Density profiles measured by a CT probe in the experiment with parameters $N_0 \approx 1.13$ s^{-1}, $Q_0 \approx 1.9$ cm^3/s and $H = 5$ cm at the beginning $t = 0$ (red line) and after a) $t \sim$5 min (red line) and b) $t \sim$1 h 5 min (red line). z_F is the depth where the buoyancy flux is zero, z_P is the penetrative depth of the descending front. Two regions of uncontaminated fluid and portions of the profiles that have been modified from the original due to "filling box" and penetrative entrainment processes are marked in a).

used to detect level z_P (see section 2.1).

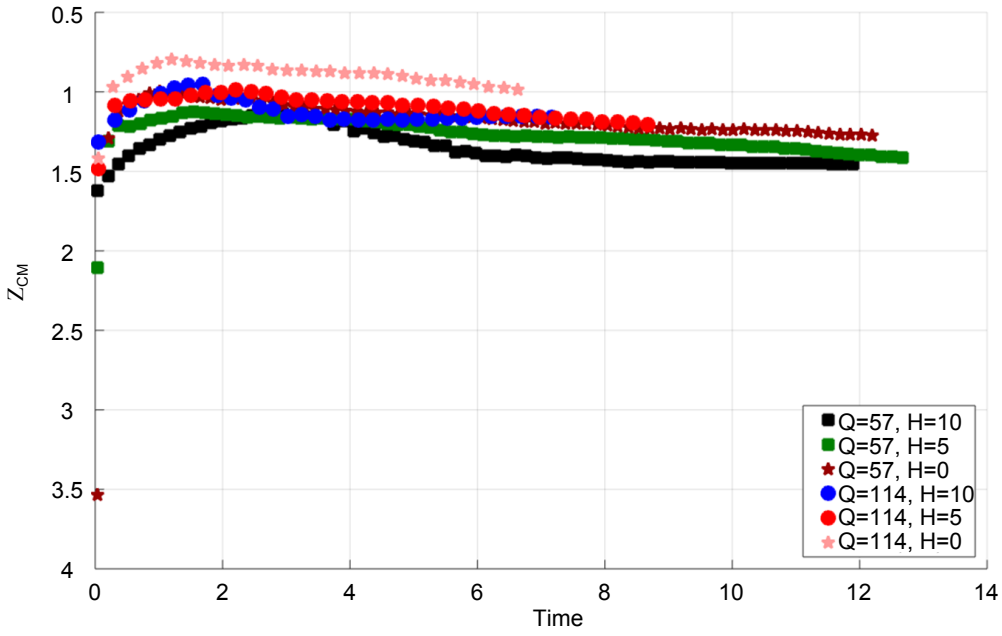

Figure 5: Non-dimensional center of mass versus non-dimensional time across the set of experiments. The nondimensionalization is discussed in section 3.1. For each experiment the flow rate (Q, in cm^3/s) and height of the mixed layers (H, in cm) are shown in the legend. $H = 0$ means linear stratification.

3 Numerical Model

3.1 Formulation of the model

To model the dynamics of the plume in a layered stratified environment we use the theory of turbulent buoyant plumes [10]. Consider conservation equations of mass, momentum and buoyancy averaged over a horizontal cross-section for a steady plume

$$\frac{dQ}{dz} = 2\epsilon_p M^{1/2} \tag{2a}$$

$$\frac{dM}{dz} = \frac{FQ}{M} \tag{2b}$$

$$\frac{dF}{dz} = -QN^2, \tag{2c}$$

where πQ is volume flux, πM is specific momentum flux and πF is buoyancy flux. Buoyancy frequency is defined as

$$N^2 = -\frac{g}{\rho_{ref}}\frac{d\overline{\rho}}{dz}.$$

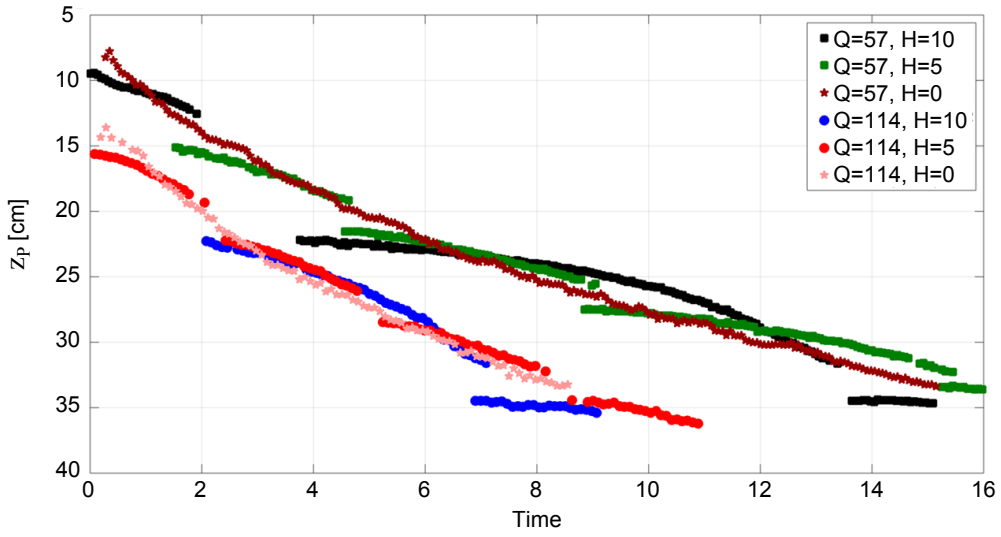

Figure 6: Penetration level (z_P) versus non-dimensional time across the set of experiments. The nondimensionalization is discussed in section 3.1. For each experiment the flow rate (Q, in cm^3/s) and height of the mixed layers (H, in cm) are shown in the legend. $H = 0$ means linear stratification.

where $\frac{d\bar{\rho}}{dz}$ is background bulk density gradient over the staircase.

Following [6] we use a characteristic length scale of the plume height $H_p = (2\epsilon_p)^{-1/2} F_s^{1/4} N_0^{-3/4}$, where ϵ_p is the entrainment constant, F_s is the source specific buoyancy flux, and N_0 is the Brunt–Väisälä frequency determined using the bulk density gradient over a staircase, to nondimensionalize variables as

$$\hat{z} = \frac{z}{H_p} \tag{3a}$$

$$\hat{N} = \frac{N}{N_0} \tag{3b}$$

$$\hat{F} = \frac{F}{F_s} \tag{3c}$$

$$\hat{Q} = \frac{Q}{(2\epsilon_p)^{4/3} F_s^{1/3} H_p^{5/3}} \tag{3d}$$

$$\hat{M} = \frac{M}{(2\epsilon_p)^{2/3} F_s^{2/3} H_p^{4/3}}. \tag{3e}$$

$$\hat{t} = \frac{t}{(2\epsilon_p)^{4/3} F_s^{1/3} H_p^{2/3} A^{-1}}, \tag{3f}$$

where A is a cross section of the basin. The buoyancy flux at the source can be computed using the $F_s = g'_p Q_s$, where πQ_s is the source flow rate and $g'_p = g(\rho_p - \rho)/\rho$ is the reduced

gravity with ρ_p being a density of the plume source fluid. The non-dimensional governing equations are then

$$\frac{d}{d\hat{z}}\hat{Q} = \hat{M}^{1/2} \tag{4a}$$

$$\hat{M}\frac{d}{d\hat{z}}\hat{M} = \hat{F}\hat{Q} \tag{4b}$$

$$\frac{d}{d\hat{z}}\hat{F} = -\hat{Q}\hat{N}^2. \tag{4c}$$

In case of a staircase, it is simplest to construct the model such that equations (4) are evaluated in the mixed layers (letting $N = 0$) and at each interface the buoyancy flux is adjusted as $\hat{F}_{i+1} = \hat{F}_i - \hat{g'}_{i,i+1}\hat{Q}_i$, where $\hat{g'}_{i,i+1}$ is the reduced gravity between two adjacent layers i and $i+1$, and $\hat{Q}_{i,i+1}$ is the volume flux at the interface (all notations are defined in Figure 10). Therefore, we solve the system of equations (4) with the number of the equations equal to the number of a mixed layers in a staircase.

3.2 Model output

Solutions of the equations (4) with initial conditions $Q_s \approx 0$, $M_s \approx 0$ and $F_s = 1$ show that z_M is almost insensitive to the height of a mixed layer (H) when $H < 1.8$ and proportional to the layer height for $H > 1.8$ (Figure 8, 9). The regime shift occurs when the buoyancy flux becomes negative at the very first interface (e.g., see Figure 8d), because in this case regardless of the height of the layer, the plume always reaches the base of the first layer and then overshoots the interface to decrease its momentum to zero. Since the buoyancy flux is constant within the mixed layer and reduces by a finite amount at the interface, the buoyancy flux profile also has a staircase structure. Given this, z_F always equals to the height of one of the interfaces and in the occasions when a plume looses its buoyancy flux within the very first layer, z_F is equal to the layer height. Thus, in Figure 9b) we observe a linear trends with the coefficient of proportionality 1, 2, 3, etc. starting from the most right line.

In our experiment, however, the plume is time-dependent and in a confined basin. Therefore, over the course of the experiment, the background stratification continuously changes due to the "filling box" and penetrative entrainment processes (as discussed in section 2.2.1). To account for the "filling box" process we use a numerical scheme proposed by [7]. In this case, from a conservation of volume in the environment we can compute the location of the top interface of the newly formed layer as $h_{i,j} = h_{i,i+1} - \hat{Q}_{i,i+1}\Delta t$, where h_i is the position of the interface that corresponds to z_F, $\hat{Q}_i$ is the volume flux at this interface and Δt is a time increment in integration. Penetrative entrainment can be also described in terms of formation of a new layer beneath z_F. In this case we assume that the entrained volume flux is linearly proportional to the volume flux of the plume at z_F [9, 4] and the height of the interface beneath z_F can be found from $h_{j,i+1} = h_{i,i+1} + E\hat{Q}_{i,i+1}\Delta t$ (indecies here are counted from the plume source, i.e., $i+1$ is located further from the source compared to j as shown in Figure 10), where E is an empirically determined constant. The density of this layer depends on how many interfaces (layers) are swept be the plume during the overshooting, and it can be computed as a weighted mean. Subsequently, these two constructed

layers are mixed to generate one mixed layer that is added to the original staircase. During this process, one "old" interface $(i, i+1)$ is being replaced by two new interfaces (i, j) and $(j, i+1)$. This leads to an additional equation in the system (4). When the depth of a generated layer is smaller than a chosen threshold l, then this layer collapses; in this case the background density is redistributed whereas the number of equations remains the same. Note also that if a generated layer via the penetrative entrainment process is more dense than a layer below, this causes merging.

In this model we have three turning parameters: side entrainment coefficient ϵ_p, penetrative entrainment coefficient E and a threshold value for layer collapsing l. To find the best combination of these parameters we choose to simulate the experiment with $N_0 \approx 1.13$ s^{-1}, $Q_0 \approx 1.9$ cm^3/s and $h = 5$ cm that clearly shows uncontaminated layers. As described in section 2.1, during the setup processes it was hard to obtain very thin interfaces, and the generated staircases, in fact, are a combination of mixed layers and regions with linear stratification. Thus, to obtain the most realistic model output and compare it with the observations we initialize the model with an experimental profile at time $t = 0$, that has been divided into a number of mixed layers with various heights (i.e., many thin layers in place of an interface, see Figure 11).

Having explored the range of parameters, we concluded that the model with $\epsilon_p = 0.08$, $E = 0.09$ and $l = 0.1$ cm (this value was non-dimensionalized correspondingly to use in a model) has the best representation of the observed physical processes. Figure 11 indicates that the model generates uncontaminated layers and modifies the background density profile due to the penetrative entrainment and the shape of the profile from the model output resembles that from the experiment.

4 Results and Discussion

From the experiments we concluded that the rate of penetration in the layered stratification depends on the location within the staircase, however, overall it follows the penetration rate that is characteristic for the linear stratification. Position of center of mass does not depend whether density profile is linear or consists of layers. The major difference between linear and staircase stratification is that in the second case uncontaminated layers are generated during the first stages of the experiment. CT measurements also show that structure of the density profiles for three examined stratification (layered with 5 and 10 cm layer depth and linear but with the same bulk density gradient) at any particular instant is very different (Figure 7).

Despite this similarity between the model output and observed profiles, further analysis of the numerical simulations has revealed that the model and experimental results differ significantly when penetration depth and location of center of mass are considered. The possible explanation can be in oversimplified parametrization of the penetrative entrainment process. To improve it, one can construct more realistic model where generated layers do not necessary ascend all the way till z_F, causing further merging, instead, these layers spread out at the level of neutral buoyancy. Further, relative contribution of the layers (covered during the overshooting) to the density can be accounted for if the total volume flux $(E\hat{Q}_{i,i+1})$ is distributed over the layers proportionally to their depths and distance from

z_F. Another possible source of error is the effect of internal waves on momentum reduction at the interfaces that is completely neglected in the current version of the model.

This study has demonstrated that although layered stratification in comparison to the linear stratification does not influence the bulk properties (penetration depth, location of center of mass), the profile structure is very different. The distinctive difference between the layered and linear stratification is in the presence of the uncontaminated layers in case of the initial layered stratification.

5 Acknowledgments

I would like to thank Colm-cille Caulfield for giving me the chance to work on this problem and providing continuous supervision throughout the summer. The GFD laboratory at WHOI provided invaluable technical support and I am very grateful to Anders Jensen, who has helped me a lot with laboratory set-up. I would like to thank John Wettlaufer for his technical advises and Karl Helfrich for helping me with data acquisition. I also would like to thank Mary-Louise Timmermans for a lot of insightful discussions. Paolo Luzzatto-Fegiz is thanked for providing the traverse operation codes and I appreciate many helpful suggestions that came from former GFD fellows Georgy Manucharyan, Srikanth Toppaladoddi and Andrew Wells.

References

[1] Knut Aagaard, JH Swift, and EC Carmack, *Thermohaline circulation in the arctic mediterranean seas*, Journal of Geophysical Research: Oceans (1978–2012), 90 (1985), pp. 4833–4846.

[2] Anna Akimova, Ursula Schauer, Sergey Danilov, and Ismael Núñez-Riboni, *The role of the deep mixing in the storfjorden shelf water plume*, Deep Sea Research Part I: Oceanographic Research Papers, 58 (2011), pp. 403–414.

[3] WD Baines and JS Turner, *Turbulent buoyant convection from a source in a confined region*, Journal of Fluid mechanics, 37 (1969), pp. 51–80.

[4] DJ Bower, CP Caulfield, SD Fitzgerald, and AW Woods, *Transient ventilation dynamics following a change in strength of a point source of heat*, Journal of Fluid Mechanics, 614 (2008), pp. 15–37.

[5] Silvana S. S. Cardoso and Andrew W. Woods, *Mixing by a turbulent plume in a confined stratified region*, Journal of Fluid Mechanics, 250 (1993), pp. 277–305.

[6] CP Caulfield and Andrew W Woods, *Turbulent gravitational convection from a point source in a non-uniformly stratified environment*, Journal of Fluid Mechanics, 360 (1998), pp. 229–248.

[7] AE Germeles, *Forced plumes and mixing of liquids in tanks*, Journal of Fluid Mechanics, 71 (1975), pp. 601–623.

[8] John Illingworth and Josef Kittler, *A survey of the hough transform*, Computer vision, graphics, and image processing, 44 (1988), pp. 87–116.

[9] YJP Lin and PF Linden, *The entrainment due to a turbulent fountain at a density interface*, Journal of Fluid Mechanics, 542 (2005), pp. 25–52.

[10] BR Morton, Geoffrey Taylor, and JS Turner, *Turbulent gravitational convection from maintained and instantaneous sources*, in Proceedings of the Royal Society of London A: Mathematical, Physical and Engineering Sciences, vol. 234, The Royal Society, 1956, pp. 1–23.

[11] Andrew Wells and Samuel Magorrian, *Turbulent plumes from ice melting into a linearly stratified ocean*, Bulletin of the American Physical Society, 60 (2015).

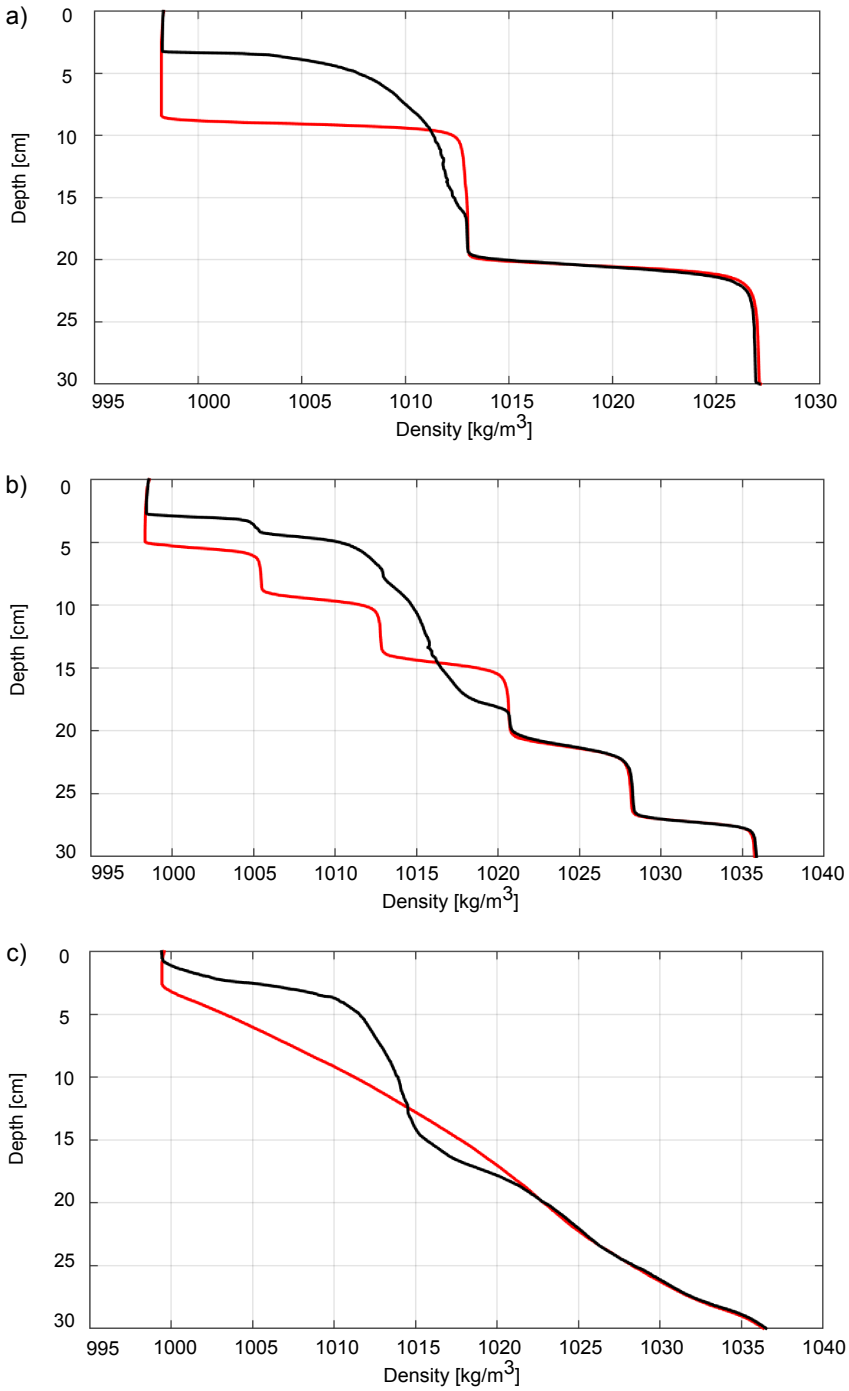

Figure 7: Density profiles measured by a CT probe in the experiment with parameters $N_0 \approx 1.13$ s^{-1}, $Q_0 \approx 1.9$ cm^3/s and various layer height a) $H = 10$ cm, b) $H = 5$ cm and c) linear stratification. Red line shows the initial profiles, black line shows the profiles after 8 min from the beginning of the experiment.

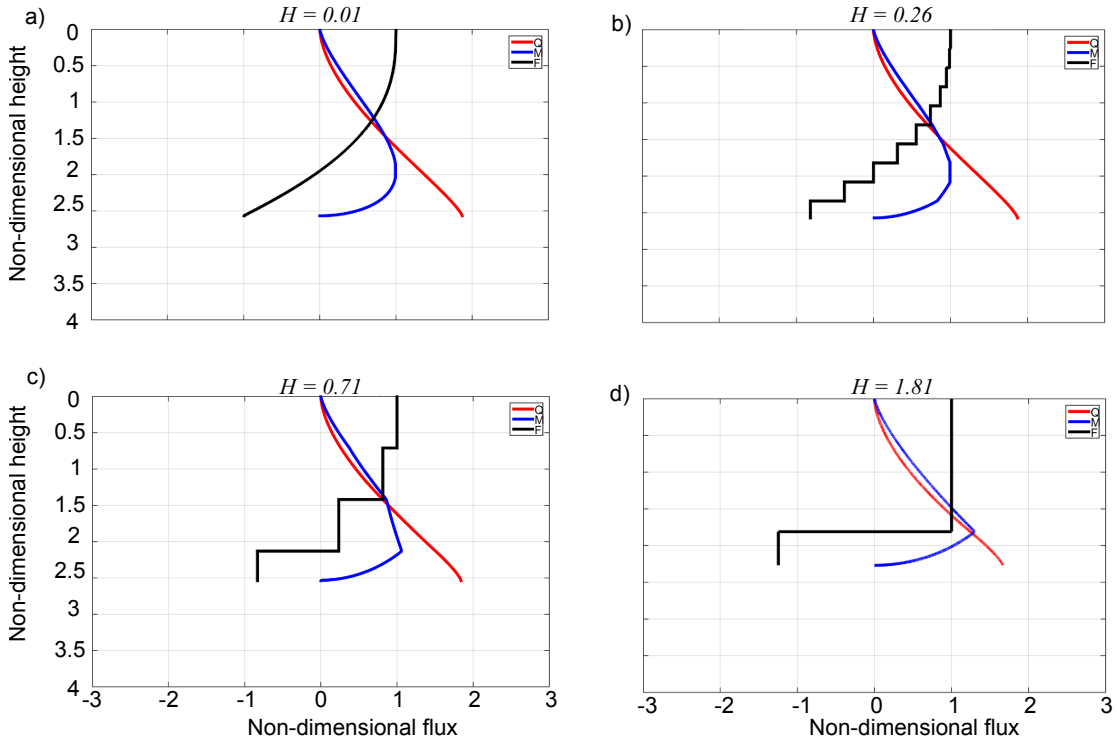

Figure 8: Solution of the equations (4) for volume flux (red), momentum flux (blue) and buoyancy flux (black) applying different non-dimensional height of the layers in a staircase a) $H = 0.01$, b) $H = 0.26$, c) $H = 0.71$ and d) $H = 1.81$. All fluxes are non-dimensional according to (3). Plume source is located at the top of the domain. Initial conditions are $Q_s \approx 0$, $M_s \approx 0$ and $F_s = 1$. All simulations were performed applying the same initial bulk density gradient.

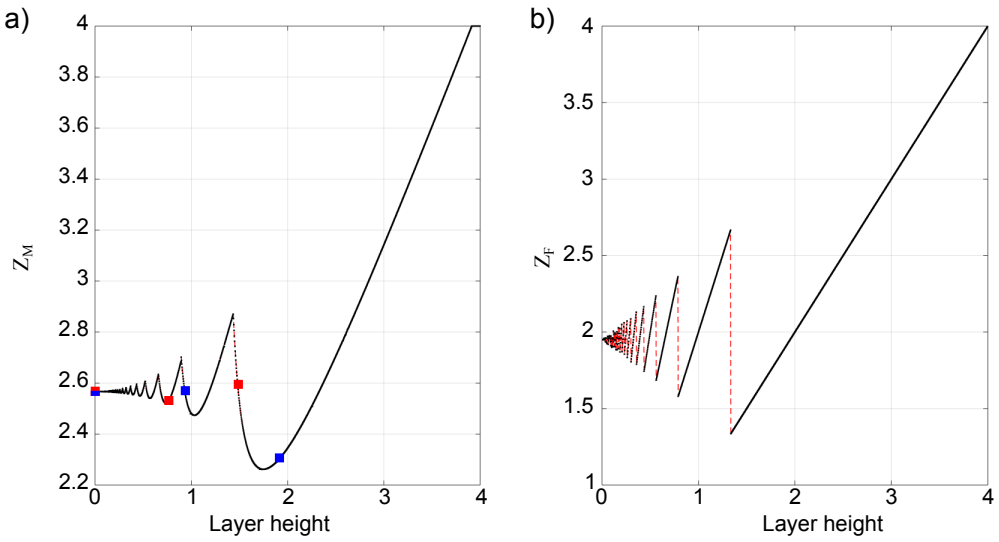

Figure 9: Dependence of a) z_M and b) z_F on nondenominational layer height. In a) red squares show the experiments with $Q_0 \approx 1.9$ cm^3/s and blue squares show the experiments with $Q_0 \approx 0.95$ cm^3/s. The red-blue square represents two experiments with the linear stratification (layer height is zero) and two different flow rates (specified above). Red dashed line serves as a connection line between data points.

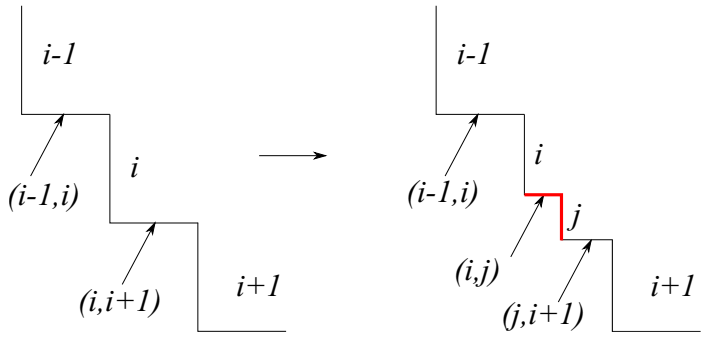

Figure 10: Schematic showing all notations using in description of a new mixed layer (red) generation due to "filling box" and penetrative entrainment processes. All layers are defined by a single index, all interfaces are defined by two indecies of the adjacent layers.

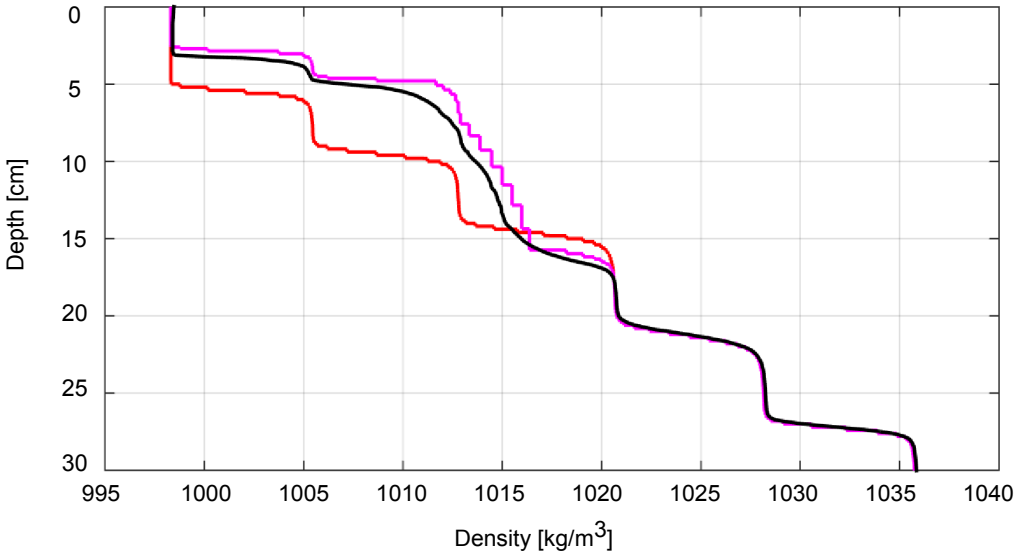

Figure 11: Density profiles measured by a CT probe in the experiment with parameters $N_0 \approx 1.13$ s^{-1}, $Q_0 \approx 1.9$ cm^3/s and $H = 5$ cm. Red line shows the initial profile that has been split into a number of mixed layers to serve as a model input, black line shows the measured profile after $\sim$7 min from the beginning of the experiment, and magenta line shows the model output after $\sim$7 min of model time.